Modeling and Simulation of Hairy Root Growth

Peter Bastian[1], Jenny Bauer[4], Andrés Chavarría-Krauser[2], Christian Engwer[1], Willi Jäger[2], Sven Marnach[3], Mariya Ptashnyk[2], and Bernhard Wetterauer[4]

[1] IWR, Universität Heidelberg, INF 368, 69120 Heidelberg, Germany (now at[3])
{peter.bastian,christian.engwer}@ipvs.uni-stuttgart.de
[2] IAM, Universität Heidelberg, INF 294, 69120 Heidelberg, Germany
{andres.chavarria.krauser,jaeger,
mariya.ptashnyk}@iwr.uni-heidelberg.de
[3] IPVS, Universität Stuttgart, Universitätsstraße 38, 70569 Stuttgart, Germany
sven.marnach@ipvs.uni-stuttgart.de
[4] IPMB, Universität Heidelberg, INF 364, 69120 Heidelberg, Germany
jenny_bauerbiol@yahoo.de, bernhard.wetterauer@urz.uni-heidelberg.de

Summary. A multiscale approach is presented to model growth of hairy roots. On the macroscopic scale, a continuous model is derived, which includes growth and nutrient transport. Water transport is considered on the microscopic scale. A Discontinuous Galerkin scheme for complex geometries is used to compute the permeability of root bulks. This permeability constitutes the linkage between micro- and macroscopic scale. The models are applied then to describe shaker cultures of hairy roots and simulations are compared to measurements.

1 Introduction

Plants remain a major source of pharmaceuticals and biochemicals. Many of these commercially valuable phytochemicals are secondary metabolites that are not essential to plant growth. Hairy roots, obtained from plants through transformation by *Agrobacterium rhizogenes*, produce many of the same important secondary metabolites and can be grown in relatively cheap hormone-free medium. Thus they may provide an alternative to agricultural processes to produce phytochemicals on a large scale [9, 11]. Hairy roots can be cultivated under sterile conditions either in a bioreactor or in shake flasks. The fast growing hairy roots are unique in their genetic and biosynthetic stability and are able to regenerate whole viable plants for further subculturing [6]. The yield of secondary metabolites is determined by biomass accumulation and by the level of secondary metabolite produced per unit biomass. Therefore

Fig. 1. *Ophiorrhiza mungos* and hairy root of *O. mungos*

a number of biological studies have focused on the growth process, growth dynamic, and production of secondary metabolites in bioreactors of different design [17, 10, 9].

Hairy roots of *Ophiorrhiza mungos* Linn., the Chinese camptotheca tree, are currently gaining the interest of pharmacologists, since a secondary metabolite, *camptothecin*, can be used to treat cancer diseases [26]. Camptothecin is a modified monoterpene indole alcaloid produced by *Camptotheca acuminata*, *Nothapodytes foetida*, some species of the genus *Ophiorrhiza*, *Ervatamia heyneana*, and *Merrilliodendron megacarpum* [24, 27]. In order to produce camptothecin efficiently, it is necessary to optimize the biological processes behind its biosynthesis (either in bioreactors or shaker cultures). However, to achieve this, it is essential to understand metabolism, growth and transport processes of and in root networks.

The aim of the project was to derive a mathematical model which describes growth of root networks and nutrient transport through root tissues. To describe the biological system a multiscale approach was used. The processes on macroscopic and microscopic scale are linked. Numerical solutions were compared to experimental data obtained from *O. mungos* hairy roots grown as shaker cultures. The model and numerical algorithms are general enough to describe growth and transport processes in bioreactors.

2 Biological Processes

The processes observed in a bioreactor are water transport, diffusion and transport of nutrients in medium and roots, and growth of roots. These processes are taking place on different scales, each of which contributes to the global system.

On the macroscopic level roots form a dense bulk which resembles a porous medium. This allows to use well known modeling approaches to describe porous media. The root bulk is hence treated as a continuous medium of

varying porosity, and all processes are defined on this continuum. Growth and nutrient transport are observed on the macroscopic scale and described through distributions. Growth is assumed to depend on nutrient concentration in the medium and inside the roots [20, 10, 21]. Three processes are responsible for changes in the mediums nutrient concentration: uptake on the root surface, convection due to pressure gradients and diffusion arising from concentration gradients. The macroscopic diffusion coefficient and the uptake kinetics depend on the density of the root network and are defined phenomenologically.

On the microscopic scale the root structure influences flow and transport processes around the root network, which has a complex highly ramified structure. The surface of a single root is covered with fine hairs, reducing conductivity [16]. Here it becomes clear that the microscopic structure determines substantially the macroscopic properties, in particular porosity and permeability.

Nutrient transport inside the roots is also a microscopic process. Since transport inside the root network is substantially faster in comparison to growth and branching, it is legitimate to consider only the average internal nutrient concentration and use a macroscopic internal nutrient concentration.

3 Macroscopic Model

Two densities are used to describe growth of hairy root networks: the root volume per unit volume ρ ($0 \leq \rho(\mathbf{x}, t) \leq 1$) and the cross section area of tips per unit volume n ($n(\mathbf{x}, t) \geq 0$). Growth can then be assumed to occur due to tip movement (elongation), tip formation (branching), and secondary thickening. Thus the change of density n is defined by a transport equation with growth velocity $\mathbf{v}$ and a branching term f. A similar approach has been used to model growth of fungi mycelia [7, 4]. The change of root density ρ is determined by the root volume produced due to tip movement. Secondary thickening is defined phenomenologically as a production term in the equation for ρ. Growth velocity and branching kinetics depend on the concentration of nutrients in the medium (denoted by $c(\mathbf{x}, t)$) and within the roots (denoted by $s(\mathbf{x}, t)$).

The transport of nutrients in the medium is defined by a convection-diffusion equation with a reaction term describing the active and passive nutrient uptake on the roots surface. Active uptake is assumed to be unidirectional (into the root network) and dependent only on the local medium nutrient concentration c. Passive uptake depends on the nutrient gradient between medium and roots, given by the difference $c - s$. Four processes which change the total internal nutrients $S = s\,V_r$, where $V_r(t)$ is the root volume, are considered here: uptake, growth, ramification and metabolism.

The precise formulation of the macroscopic model of hairy root growth reads

$$\begin{aligned}
&\partial_t n + \nabla \cdot (n\,\mathbf{v}) = f && \text{in } (0,T)\times\Omega,\\
&\partial_t \rho = n\,\|\mathbf{v}\| + q && \text{in } (0,T)\times\Omega,\\
&\partial_t\left((1-\rho)c\right) + \nabla\cdot(\mathbf{u}\,c) - \nabla\cdot(D_c(1-\rho)\nabla c) = -g && \text{in } (0,T)\times\Omega,\\
&\tfrac{d}{dt}S = \int\limits_{\Omega} g\,dx - \gamma_g \int\limits_{\Omega} (n\,\|\mathbf{v}\| + q)\,dx - \gamma_r \int\limits_{\Omega} f\,dx - \gamma_m\, S && \text{in } (0,T),
\end{aligned} \tag{1}$$

with

$$\begin{aligned}
\mathbf{v} &= R\,s\,(\rho_{max}-\rho)\,(\nabla\mu + \alpha_\tau \boldsymbol{\tau})\,,\\
\nabla\mu &= \alpha_c\nabla c - \alpha_\rho\nabla\rho - \alpha_n\nabla n\,,\\
q &= \chi\,s\,\rho\,(\rho_{max}-\rho)\,,\\
f &= \beta\,c\,s\,\rho\,(\rho_{max}-\rho)\,,\\
g &= \frac{2\lambda\,n}{r}\,\rho\,(\,K_m\,c + P\,(c-s))\,,
\end{aligned}$$

where R is a growth rate, ρ_{max} is the maximal root density, χ is a secondary thickening rate, β is a branching rate, λ is the characteristic length of the uptake-active tissue around a tip, K_m is a constant describing active uptake rate, P is a permeability characterizing passive uptake, $\mathbf{u}$ is the flow velocity of the medium, D_c is a diffusion constant, and γ_g, γ_r and γ_m are constants describing the proportion of metabolites used for growth, ramification and metabolism, respectively. Since hairy roots are agravitropic [14] growth velocity can be assumed to be independent of gravity. Growth can then be presumed to occur along nutrient gradients and away from dense tissue. Pure densification of the root system is modeled by the local rotation $\boldsymbol{\tau}$, which is a unit vector orthogonal to $\nabla\mu$ and ∇n. It does not affect the density distribution of tips, although mass is still produced and ρ changes. Here α_c, α_ρ, α_n, and α_τ are phenomenological constants, which relate the growth driving gradients to the resulting growth velocity.

Initial density distributions and nutrient concentrations are prescribed. For both the bioreactor and the shake flasks the side walls of the reactor vessel (Γ_{sw}) are impermeable to the medium. In the bioreactor we have inflow (Γ_{in}) and outflow (Γ_{out}) boundaries. On Γ_{in} the nutrient concentration is given and Dirichlet boundary condition can be posed. On Γ_{out} we have outflow boundary condition. In the case of the shaker cultures no-flux boundary condition can be posed (i.e. $\partial\Omega = \Gamma_{sw}$ and $\Gamma_{in} = \Gamma_{out} = \emptyset$). Since roots cannot extend beyond the vessel, the tip density fulfills also the no-flux boundary conditions.

$$\begin{aligned}
&n(0,\mathbf{x}) = n_0(\mathbf{x}), \rho(0,\mathbf{x}) = \rho_0(\mathbf{x}) && \text{in} \quad \Omega,\\
&c(0,\mathbf{x}) = c_0, S(0) = S_0, && \text{in} \quad \Omega,\\
&n\,\mathbf{v}\cdot\boldsymbol{\nu} = 0 && \text{on} \quad (0,T)\times\partial\Omega,
\end{aligned}$$

$$\begin{aligned} c &= c_D && \text{on} \quad (0,T)\times \Gamma_{\text{in}},\\ D_c(1-\rho)\,\nabla c - \mathbf{u}\,c)\cdot\boldsymbol{\nu} &= 0 && \text{on} \quad (0,T)\times \Gamma_{\text{out}},\\ \nabla c\cdot\boldsymbol{\nu} &= 0 && \text{on} \quad \Gamma_{sw}\,. \end{aligned}$$

The water velocity $\mathbf{u}$ is defined by Darcy's law. We distinguish between Dirichlet condition given by pressure values on the boundary Γ_D and Neuman conditions defined by flux through the boundary Γ_N. Depending on the experimental setup, either Neumann or Dirichlet conditions are posed on Γ_{in} and Γ_{out}. For a shake flask and on the sidewalls (Γ_{sw}) of a bioreactor, no-flux (i.e. homogeneous Neumann) conditions need to be posed.

$$\begin{aligned} \nabla\cdot\mathbf{u} &= 0 && \text{in} \quad \Omega,\\ \mathbf{u} &= -K\nabla p && \text{in} \quad \Omega,\\ p &= p_0 && \text{on} \quad \Gamma_D\subset\partial\Omega,\\ \mathbf{u}\cdot\boldsymbol{\nu} &= j && \text{on} \quad \Gamma_N=\partial\Omega\setminus\Gamma_D\,. \end{aligned} \tag{2}$$

Here K is the permeability function of the root network. On the macroscopic scale K changes with density, but derivation of the relation is cumbersome if not impossible for general geometries. It must be computed hence for a certain structure on the microscopic scale.

The effective permeability K is assumed to be of the form

$$K = K_0\cdot K_{\text{rel}}, \tag{3}$$

where K_0 is the average coefficient relating the flow velocity $\mathbf{u}$ to the pressure gradient ∇p in an empty reactor ($\rho = 0$). $K_{\text{rel}}(\rho)$ a dimensionless relative permeability which reflects the local root structure. K_0 can be obtained by determining the Hagen–Poiseuille flow in the reactor, while K_{rel} is computed using simulations of the microscopic model.

4 Microscopic Model

On the microscopic scale we consider water flow between single root branches. To simplify the problem, we assume an incompressible potential flow:

$$\begin{aligned} \nabla\cdot\mathbf{u} &= 0 && \text{in} \quad \Omega,\\ \mathbf{u} &= -\nabla p && \text{in} \quad \Omega,\\ p &= p_0 && \text{on} \quad \Gamma_D\subset\partial\Omega,\\ \nabla p\cdot\boldsymbol{\nu} &= j && \text{on} \quad \Gamma_N=\partial\Omega\setminus\Gamma_D\,. \end{aligned} \tag{4}$$

The domain Ω has a complex geometry, given by the root structure. Water uptake by the roots (growth) is small compared to the water flow, therefore Neumann boundary conditions with $j = 0$ can be assumed on the root surfaces.

4.1 Numerical Methods for Microscale Simulations

The root structure on the microscopic scale exhibits a complex shape. Classical numerical methods require a grid resolving such complex geometries. Creating these grids is a very sophisticated process and generates a high number of unknowns. We developed a discretization scheme for complex geometries, based on a Discontinuous Galerkin (DG) discretization on a structured grid and a structured grid for the construction of trial and test functions [8]. This method offers a discretization where the number of unknowns is not directly determined by the possibly very complicated geometrical shapes, but still allows the provision of fine structures, even if their size is significantly smaller than the grid cell size.

Let $\Omega \subseteq \mathbb{R}^d$ be a domain. On a sub-domain $\Omega^* \subseteq \Omega$ we want to solve Eqn. (4). The shape of Ω^* is usually based on geometrical properties retrieved from experiments, like micro-CT images, or from computations. $\mathcal{T}(\Omega) = \{E_0, \ldots, E_{M-1}\}$ is a partitioning, where the mesh size $h = \min\{\operatorname{diam}(E_i) \mid E_i \in \mathcal{T}\}$ is not directly determined by the geometrical properties. Nevertheless error control on solution of the partial differential equation might require a smaller h due to the shape of $\partial\Omega$. For Ω^* a triangulation based on $\mathcal{T}(\Omega)$ is defined $\mathcal{T}(\Omega^*) = \{E_n^* |\ E_n^* = \Omega^* \cap E_n \wedge E_n^* \neq \emptyset\}$, see Fig. 2. As E_n^* is always a subset of E_n we will call E_n fundamental element of E_n^*. The internal skeleton Γ_{int} and external skeleton Γ_{ext} of the partitioning are denoted by

$$\Gamma_{\text{int}} = \left\{ \gamma_{e,f} = \partial E_e^* \cap \partial E_f^* \;\middle|\; E_e^*, E_f^* \subset \Omega^* \text{ and } E_e^* \neq E_f^* \text{ and } |\gamma_{e,f}| > 0 \right\},$$
$$\Gamma_{\text{ext}} = \left\{ \gamma_e = \partial E_e^* \cap \partial\Omega^* \mid E_e^* \subset \Omega^* \text{ and } |\gamma_{e,f}| > 0 \right\}.$$

In the finite element mesh $\mathcal{T}(\Omega^*)$ each element E_n^* can be shaped arbitrarily. Using DG, unlike conforming methods, the shape functions can be chosen in-

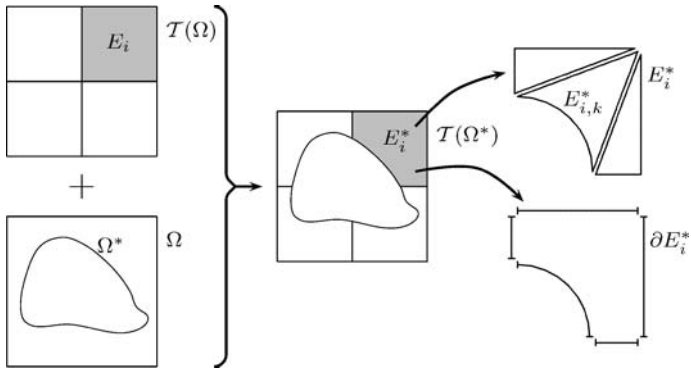

Fig. 2. Construction of the partitions $\mathcal{T}(\Omega^*)$ from the partitions $\mathcal{G}$ and $\mathcal{T}$ of the domain Ω and of E^* from its fundamental element and Ω^*. The local triangulation of E_i^* and ∂E_i^*

dependently from the shape of the element. Note that certain DG formulations are especially attractive, because they are element wise mass conservative and therefore able to accurately describe fluxes over element boundaries. We use a DG formulation with local base functions $\varphi^*_{n,j}$ being polynomial functions $\varphi_{n,j} \in P_k$ defined on the fundamental element E_n, with their support restricted to E^*_n:

$$\varphi^*_{n,j} = \begin{cases} \varphi_{n,j} & \text{inside of } E^*_n \\ 0 & \text{outside of } E^*_n \end{cases}, \tag{5}$$

$P_k = \{\varphi : \mathbb{R}^d \to \mathbb{R} \mid \varphi(x) = \sum_{|\alpha| \le k} c_\alpha x^\alpha\}$ is the space of polynomial functions of degree k and α a multi–index. The resulting finite element space is defined by

$$V^*_k = \left\{ v \in L_2(\Omega^*) \,\middle|\, v|_{E^*_n} \in P_k \right\} \tag{6}$$

and is discontinuous on the internal skeleton Γ_{int}. With each $\gamma_{e,f} \in \Gamma_{\text{int}}$ we associate a unit normal n. The orientation can be chosen arbitrarily, in this implementation we have chosen n oriented outwards E^*_e for $e > f$ and inwards otherwise. With every $\gamma_e \in \Gamma_{\text{ext}}$ we associate n oriented outwards Ω^*. The jump $[\,.\,]$ and the average $\langle\,.\,\rangle$ of a function $v \in V^*_k$ at $x \in \gamma \in \Gamma_{\text{int}}$ are defined as

$$[\,v\,] = v|_{E^*_e} - v|_{E^*_f} \qquad \text{and} \qquad \langle\,v\,\rangle = \frac{1}{2}\left(v|_{E^*_e} + v|_{E^*_f}\right).$$

Assembling the local stiffness matrix in DG requires integration over the volume of each element E^*_n and its surface ∂E^*_n. Integration is done using a local triangulation of E^*_n. E^*_n is subdivided into a disjoint set $\{E^*_{n,k}\}$ of simple geometric objects, i.e. simplices and hypercubes, with $\bar{E}^*_n = \bigcup_k \bar{E}^*_{n,k}$, see Fig. 2.

The integral over a function f on E^*_n can then be evaluated as

$$\int_{E^*_n} f(x)\, dx = \sum_k \int_{E^*_{n,k}} f(x)\, dx,$$

where $\int_{E^*_{n,k}} f\, dx$ is evaluated using standard quadrature rules.

4.2 Numerical Estimation of Macroscopic Parameters from Microscopic Simulations

Following the approach described in the previous subsection and applying this method to the microscopic problem in (4), the relative permeability, as introduced in (3), can be computed from direct simulation of flow through a root bulk:

$$K_{\text{rel}} = \left(\int_{\Gamma_{\text{in}}} \mathbf{u} dx \right) \cdot \left(\int_{\Gamma_{\text{in}}} \frac{p_2 - p_1}{h} dx \right)^{-1}, \tag{7}$$

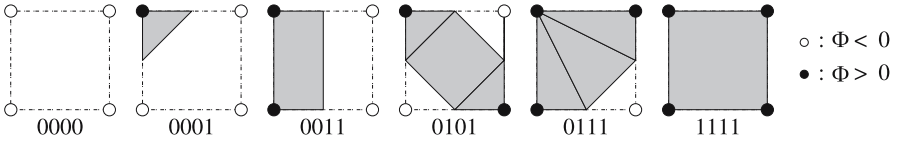

Fig. 3. The Marching Cube algorithm in $\mathbb{R}^2$ distinguishes six basic cases, depending on the value of a function Φ in the corners. The pictures show these six different cases, together with their key in the look-up table

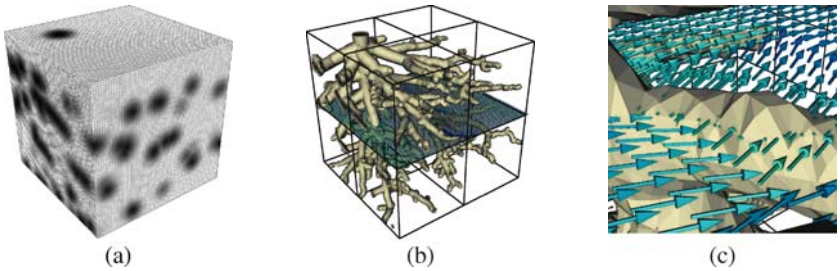

Fig. 4. (**a**) shows the scalar function describing the geometry, the marching simplex algorithm yields the geometry visible in (**b**). Pressure and velocity are computed on the given domain, using direct simulations with a Discontinuous Galerkin scheme. The resulting velocity can be seen in (**b**). (**c**) shows a closeup

where $\Gamma_{in} \subset \Gamma_D$ describes the inflow boundary. Dirichlet boundary conditions are posed both on the inflow and the outflow boundary.

The domain Ω^* is implicitly given by a scalar function Φ. This scalar function will usually be obtained through post processing of image data, i.e. from CT images. In these calculations we use artificially generated structures (Fig. 4.2a), based on structural parameters (using the PlantVR software [5]). The sub-domain boundary $\partial\Omega^*$ is given as an iso-surface $\Phi = 0$.

The local triangulation is based on the *Marching Cube/Simplex* Algorithm [13]. These algorithms give a surface reconstruction for an iso-surface. Each vertex of an element can be below or above the value of the iso-surface, read inside or outside the sub-domain. For a cube element in $\mathbb{R}^2$ this gives 16 different cases. Each of these cases corresponds to one of six basic cases and can be transformed using simple geometric operations (see Fig. 3). A look-up table maps each case to the appropriate surface reconstruction. The key for the look-up table is given by assigning the state of each corner (inside $\rightarrow$ 1, outside $\rightarrow$ 0) to one bit of an integer. The look-up table was extended to provide a surface and a volume reconstruction.

Using the formulation described in [18, 19], (4) reads: Find $p \in V_k^*$ such that

$$a_\epsilon(p, v) + J_{\sigma\beta}(p, v) = l_{\epsilon\sigma\beta}(v) \qquad \forall v \in V_k^*.$$

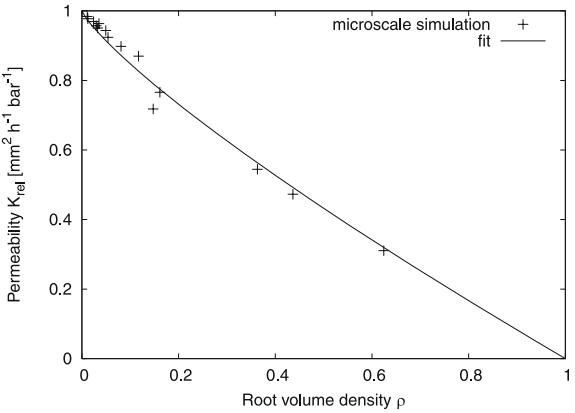

Fig. 5. Estimation of macroscale parameters from microscale simulations. Direct simulation of (4) for different root bulks with different densities yields correlation of K_{rel} and ρ. Model assumed: $K_{\mathrm{rel}} = 1 - \rho^b$, where $b = 0.82 \pm 0.02$

The bilinear form

$$\begin{aligned} a_\epsilon(p,v) = &\sum_{E_e^* \in \mathcal{T}^*} \int_{E_e^*} (K\nabla p)\cdot\nabla v \; dV \\ &+ \sum_{\gamma_{ef}\in\Gamma_{\mathrm{int}}} \int_{\gamma_{ef}} \epsilon \,\langle\,(K\nabla v)\cdot n\,\rangle[\,p\,] - \langle\,(K\nabla p)\cdot n\,\rangle[\,v\,]\; ds \\ &+ \sum_{\gamma_e\in\Gamma_{\mathrm{D}}} \int_{\gamma_e} \epsilon\,(K\nabla v)\cdot n\; p - (K\nabla p)\cdot n\; v\; ds \end{aligned}$$

is parametrized by $\epsilon = \pm 1$. Choosing $\epsilon = 1$ we get a non–symmetric scheme introduced by Oden, Babušky and Baumann in [15]. For $\epsilon = -1$ we obtain the Symmetric Interior Penalty method which needs an additional stabilization term added to the bilinear form:

$$J_{\sigma\beta}(p,v) = \sum_{\gamma_{ef}\in\Gamma_{\mathrm{int}}} \frac{\sigma}{|\gamma_{ef}|^\beta} \int_{\gamma_{ef}} [\,p\,][\,v\,] ds \; + \sum_{\gamma_e\in\Gamma_{\mathrm{D}}} \frac{\sigma}{|\gamma_e|^\beta} \int_{\gamma_e} pv \; ds$$

with $\sigma > 0$ and β, where β depends on the dimension of Ω ($\beta = 1$ when dim $= 2$). Choosing $\epsilon = 1$ and $\sigma > 0$ results in the Non–Symmetric Interior Penalty method.

The right hand side is a linear form

$$\begin{aligned} l_{\epsilon\sigma\beta}(v) = &\sum_{E_e^*\in\mathcal{T}^*} \int_{E_e^*} f\; v\; dV \; + \sum_{\gamma_e\in\Gamma_{\mathrm{N}}} \int_{\gamma_e} J\; v\; ds \\ &+ \sum_{\gamma_e\in\Gamma_{\mathrm{D}}} \int_{\gamma_e} \epsilon\,(K\nabla v)\cdot n\; g\; ds \; + \sum_{\gamma_e\in\Gamma_{\mathrm{D}}} \frac{\sigma}{|\gamma_{ef}|^\beta} \int_{\gamma_e} v\; g\; ds. \end{aligned}$$

Direct simulation of Eq. (4) for different realizations of root bulks, yields K_{rel} and ρ. K_{rel} is assumed to be of the form $K_{\mathrm{rel}}(\rho) = 1 - \rho^b$ and b is determined using a mean square fit.

Fig. 5 shows the dependence of K_{rel} on ρ and the fitted function $K_{\mathrm{rel}}(\rho)$, where $b = 0.82 \pm 0.02$.

5 Application of the Macroscopic Model

There are two common ways of cultivating hairy roots, either in shake flasks or in bioreactors. Shaker cultures are used more often because of their simple assembly and usage in experiments and biological research. However, experiments in shaker cultures do not provide information about the spatial structure and distribution of roots. Bioreactors have rather industrial applications and are more complex to operate and to use as experimental set-ups. In the work presented here both cultivation methods were considered. In fact, equations (1) are able to describe both situations, as these differ only slightly in the method used to guarantee nutrient supply. While the principle of shake flask is based on permanent shaking of medium and culture, bioreactors use medium fluxes to ensure nutrient and oxygen supply.

5.1 Simulation of Shaker Cultures

For numerical simulation Eqs. (1) can be simplified to reduce the amount of free parameters. Uptake of nutrients can be considered to be purely of active nature, neglecting the passive transport ($P = 0$). Moreover, the energy cost for branching of new tips can be neglected ($\gamma_r = 0$). Since the root branches are very thin and variation in radius is small, root thickening can be neglected as well ($\chi = 0$). The main purpose of shaking is to supply oxygen and to ensure a homogeneous distribution of nutrients. This means that transport in the medium is non-limiting to uptake and growth. In the simulation this homogeneous distribution can be achieved via large diffusion. Active water transport is neglected.

A personal computer was used to simulate the macroscopic model (1), using a implementation of the numerical schemes based on the *DUNE* framework [3, 1]. For spatial discretization of the first and third equation in (1) a cell centered finite volume scheme on a structured grid was used [12]. The diffusive and convective/reactive part of the third equation in (1) were decoupled for discretization in time (second order operator splitting [23]). To prevent both instabilities in the transport term and effects from strong numerical diffusion, the convection equation was solved using an explicit second order Godunov upwind scheme with a minmod slope limiter [25, 12]. The diffusive part of the equation was solved implicitly. The ordinary differential equations for the

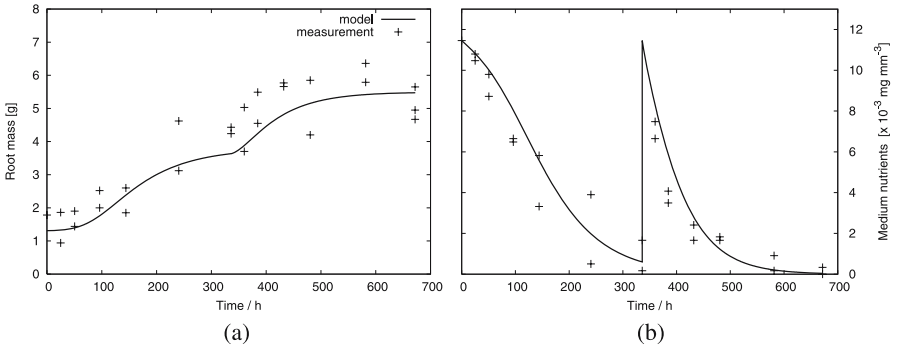

Fig. 6a,b. Comparison of simulation and experimental data from hairy roots grown as shaker cultures. The evolution in time of root mass (**a**) and concentration of sucrose in the medium (**b**) are compared to measurements. At 336 hours cultures were transferred into fresh medium

root density and the inner nutrient concentration S [second and fourth Eq. in (1)] were solved with Euler's method [22].

The parameters in the model are chosen such that the numerical results fit experimental data obtained from *O. mungos* hairy roots (Fig. 6). Gradients of nutrients and tip density, with moderate tissue compaction (local rotation), were chosen here as the driving force of growth. Very good agreement is found between measurements and simulation (mass increase: $R^2 = 0.85$, nutrient uptake: $R^2 = 0.93$). The model delivers spatial information on growth patterns as well. A simulation of a two dimensional flask is found in Fig. 7. The distributions are assumed to be constant in one of the the three dimensions. Simulation in three dimensions could however be easily implemented. Measurements deliver at the moment only data describing the kinetics of mass increase and nutrient uptake (compare Fig. 6), which do not include quantitative information on spatial patterns. Therefore, verification of the patterns in Fig. 7 is at the moment not possible. It is hence not clear which growth process dominates in the growth force $\nabla\mu + \alpha_\tau \boldsymbol{\tau}$. Do hairy roots follow rather nutrient gradients than space gradients, or is diffusion of root tips more important? Or is mass increase a consequence of tissue compaction (local rotation)? It will probably be a mixture of all and other processes not accounted for. A detailed discussion regarding this issue can be found in Bastian et al. (2007b).

5.2 Hairy Roots Bioreactor

Root growth in bioreactors can be described by the full macroscopic model (1). Active water transport has to be considered. The flow velocity $\mathbf{u}$ can be calculated using Darcy's-Law (2), which requires the permeability $K(\rho)$. The relation between K and the root volume density ρ is determined by the microscopic model (compare Fig. 5). The model and numerical algorithms are

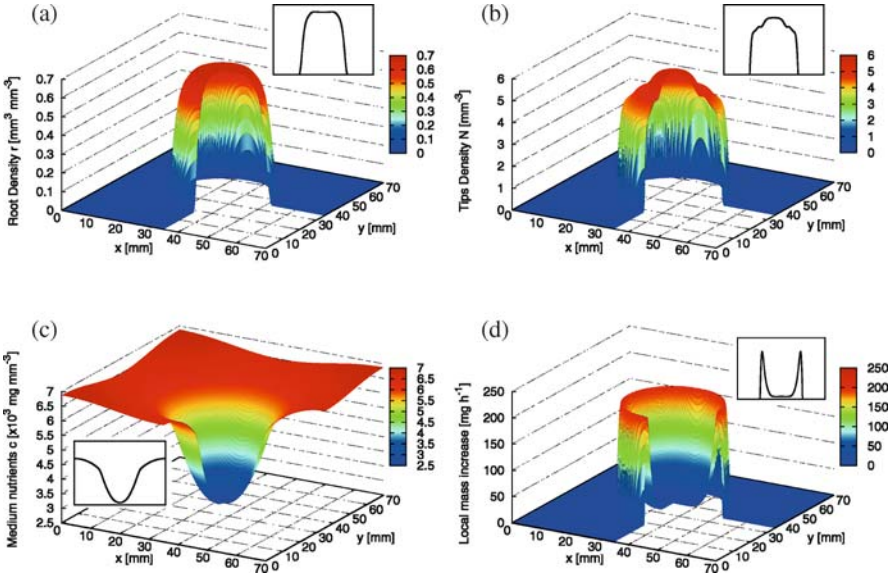

Fig. 7a–d. Simulated two dimensional spatial growth patterns of hairy roots grown as shaker cultures. (**a**) root volume density, (**b**) root tip density, (**c**) nutrient concentration in medium, and (**d**) local mass increase (all after 380 h of growth)

elaborated sufficiently to calculate and optimize the transport and growth processes in bioreactors. For meaningful simulation, parameters related to the three dimensional structure are required for (1). However these are not available from shaker culture experiments.

In order to study three dimensional growth patterns, a small experimental bioreactor (*WEWA I*) for root cultures was constructed in the group of Prof. Wink (IPMB, Universität Heidelberg) to deliver the information needed. "WEWA I"s construction is based on the *Low Cost Mist Bioreactor* (LCMB) of the company ROOTec GmbH (Heidelberg, Germany; Patentnumber: US 2003/0129743A1 / EP 1268743B1). The bioreactor system consists of a 3 l reactor reservoir (Fig. 8), a medium reservoir, a gas reservoir, and a mist chamber for the distribution of medium over the fixed root bed. Every 15 min the root inoculum is sprayed with 20 ml medium. Due to spraying, a pressure difference of 0.3 bar arises, which is used to return the surplus medium into the medium reservoir. The pressure in the reactor is controlled by a pneumatic relief valve (0.5 bar opening pressure). Instead of the B5 medium (1% sucrose; ROOTec GmbH, Heidelberg, Germany) used in shaker cultures, a modified version with 0.5% sucrose is used to obtain an optimal medium osmolarity. In order to prevent contaminations in the reactors a bacteriostatic (0.5 g/l Claforan) and a fungicide (40 mg/l Nystain) were added to the medium.

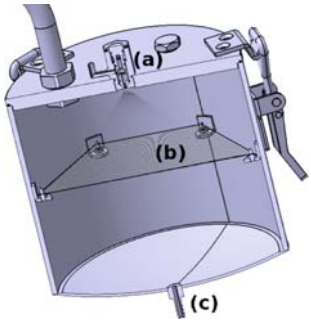

Fig. 8a–c. Scheme of the *WEWA I* mist chamber: injection valve of medium (**a**), mesh on which cultures are fixed (**b**), drain for surplus medium (**c**)

"WEWA I" is being put into operation at the moment. Several test runs have been done so far. However, these test measurements have not supplied reliable enough experimental data to identify the model parameters. Therefore meaningful simulations of the processes in bioreactors were not possible until now.

6 Conclusion

The work presented here has a general interest for modeling and simulation of complex growing networks like root systems and growth processes in bioreactors. A macroscopic model describing water and nutrient transport through a growing root network was derived. The growth of roots in a water solution and the dense growth habit of hairy roots give the possibility to define growth as a change of tissue volume density. This allows further to expand a one dimensional growth model, namely pure elongation of single roots, to a continuous three dimensional model, which delivers information on spatial growth patterns. Linkage of the microscopic and the macroscopic scale is accomplished by the elaborate and novel numerical algorithms developed for solution of elliptic equations on complex shaped domains. Comparison of numerical solutions and measurements of hairy roots shaker cultures, showed that the model is able to describe very well the kinetics of growth and nutrient uptake. Moreover, model and numerical algorithms are general enough to describe growth in bioreactors. Optimization of camptothecin production is still an open task due to the lack of experimental data. The model presented here is a good step forward towards achieving this and represents a sound base for further research. The numerical methods developed for microscale simulations are of interest for a wide range of applications, ranging from pore scale problems for water resources to cell biology. In future work these methods will be extended to time-dependent problems.

References

[1] P. Bastian, M. Blatt, A. Dedner, C. Engwer, R. Klöfkorn, R. Kornhuber, M. Ohlberger, and O. Sander. A generic grid interface for parallel and adaptive scientific computing. part ii: Implementation and tests in dune. Preprint, 2007. Submitted to *Computing*.

[2] P. Bastian, A. Chavarría-Krauser, C. Engwer, W. Jäger, S. Marnach, and M. Ptashnyk. Modelling *in vitro growth* of dense root networks. In preparation, 2007.

[3] P. Bastian, M. Droske, C. Engwer, R. Klöfkorn, T. Neubauer, M. Ohlberger, and M. Rumpf. Towards a unified framework for scientific computing. In R. Kornhuber, R.H.W. Hoppe, D.E. Keyes, J. Périaux, O. Pironneau, and J. Xu, editors, *Domain Decomposition Methods in Science and Engineering*, number 40 in Lecture Notes in Computational Science and Engineering, pages 167–174. Springer-Verlag, 2004.

[4] G. P. Boswell, H. Jacobs, F. A. Davidson, G. M. Gadd, and K. Ritz. Growth and function of fungal mycelia in heterogeneous environments. *Bulletin of Mathematical Biology*, 65:447–477, 2003.

[5] S. Chuai-Aree, S. Siripant, W. Jäger, and H.G. Bock. PlantVR: Software for Simulation and Visualization of Plant Growth Model. In *Proceedings of PMA06: The Second International Symposium on Plant growth Modeling, Simulation, Visualization and Applications*. Beijing, 2006.

[6] P. M. Doran. *Hairy Roots: Culture and Applications*. Harwood Academic Publishers, Amsterdam, 1997.

[7] L. Edelstein-Keshet. *Mathematical models in biology*. The Random House/ Birkhäuser Mathematics Series, New York, 1988.

[8] C. Engwer and P. Bastian. A Discontinuous Galerkin Method for Simulations in Complex Domains. Technical Report 5707, IWR , Universität Heidelberg, http://www.ub.uni-heidelberg.de/archiv/5707/, 2005.

[9] Y. J. Kim, P. J. Weathers, and B. E. Wyslouzil. Growth of *Artemisia annua* hairy roots in liquid and gas-phase reactors. *Biotechnology and Bioengineering*, 80:454–464, 2002.

[10] Y. J. Kim, P. J. Weathers, and B. E. Wyslouzil. Growth dynamics of *Artemisia annua* hairy roots in three culture systems. *Journal of Theoretical Biology*, 83:428–443, 2003.

[11] Y. J. Kim, B. E. Wyslouzil, and P. J. Weathers. Invited review: Secondary metabolism of hairy root cultures in bioreactors. *In Vitro Cell. Dev. Biol. Plant*, 38:1–10, 2002.

[12] Randall J. LeVeque. *Finite Volume Methods for Hyperbolic Problems*. Cambridge University Press, 2002.

[13] William E. Lorensen and Harvey E. Cline. Marching cubes: A high resolution 3d surface construction algorithm. In *SIGGRAPH '87: Proceedings of the 14th annual conference on Computer graphics and interactive techniques*, pages 163–169, New York, NY, USA, 1987. ACM Press.

[14] E. Odegaard, K. M. Nielsen, T. Beisvag, K. Evjen, A. Johnsson, O. Rasmussen, and T. H. Iversen. Agravitropic behaviour of roots of rapeseed (*Brassica napus* L.) transformed by *Agrobacterium rhizogenes*. *J Gravit Physiol.*, 4(3):5–14, 1997.

[15] J. T. Oden, I. Babuška, and C. E. Baumann. A discontinuous *hp*-finite element method for diffusion problems. *Journal of Computational Physics*, 146:491–519, 1998.

[16] M. Ptashnyk. Derivation of a macroscopic model for nutrient uptake by a single branch of hairy-roots. University Heidelberg, Preprint, 2007.

[17] D. Ramakrishnan and R. W. Curtis. Trickle-bed root culture bioreactor design and scale-up: Growth, fluid-dynamics, and oxygen mass transfer. *Biotechnology and Bioengineering*, 88(2):248–260, 2004.

[18] B. Rivière and M.F. Wheeler. Discontinuous galerkin methods for flow and transport problems in porous media. *Communications in Numerical Methods in Engineering*, 18:63–68, 2002.

[19] B. Rivière and M.F. Wheeler. A posteriori error estimates and mesh adaptation strategy for discontinuous galerkin methods applied to diffusion problems. *Computers & Mathematics with Applications*, 46(1):141–163, 2003.

[20] D. Robinson. Tansley review no. 73. The responses of plants to non-uniform supplies of nutrients. *The New Phytologist*, 127:635–674, 1994.

[21] S. R. Schnapp, W. R. Curtis, R. A. Bressan, and P. M. Hasegawa. Growth yields and maintenance coefficients of unadapted and NaCI-adapted tobacco cells grown in semicontinuous culture. *Plant Physiol*, 96:1289–1293, 1991.

[22] J. Stoer and R. Burlisch. *Numerische Mathematik 2*. Springer, 4 edition, 2000.

[23] Gilbert Strang. On the construction and comparison of difference schemes. *SIAM J. Numer. Anal.*, 5:506–517, 1968.

[24] H. Sudo, T. Yamakawa, M. Yamazaki, N. Aimi, and K. Saito. Bioreactor production of camptothecin by hairy root cultures of *Ophiorrhiza pumila*. *Biotechnology Letters*, 24:359–363, 2002.

[25] P. K. Sweby. High resolution schemes using flux-limiters for hyperbolic conservation laws. *SIAM J. Num. Anal.*, 21:995–1011, 1984.

[26] C. H. Takimoto, J. Wright, and S. G. Arbuck. Clinical applications of the camptothecins. *Biochim Biophys Acta*, 1400:107–119, 1998.

[27] M. Wink, A. W. Alfermann, R. Franke, B. Wetterauer, M. Distl, J. Windhövel, O. Krohn, E. Fuss, H. Garden, A. Mohagheghzadeh, E. Wildi, and P. Ripplinger. Sustainable bioproduction of phytochemicals by plant in vitro cultures: anticancer agents. *Plant Genetic Resources. NIAB.*, 3(2):90–100, 2005.